Inorg. Chem. **2005**, *44*, 7443–7448

Evidence of Incipient Bond-Stretching Isomerism in $Sr_{2.04(1)}Ca_{0.96(1)}Sn_5$ from Variable-Temperature Structural Studies

Shalabh Gupta and Ashok K. Ganguli*

Department of Chemistry, Indian Institute of Technology, Delhi, Hauz Khas, New Delhi, 110016

Received May 2, 2005

The title compound was found to crystallize in the Pu_3Pd_5 structure type (SG *Cmcm*) with cell dimensions of $a = 10.5179(9)$ Å, $b = 8.4789(8)$ Å, and $c = 10.7623(10)$ Å. The structure consists of isolated Sn_5^{6-} square-pyramidal units surrounded by cations that seem to play a crucial role in stabilizing the Zintl polyanions. The square pyramids contract at low temperatures (100 K) leading to the shortening of the basal intracluster Sn–Sn bond (2.74 Å), while the intercluster bonds become very large, indicating features of bond stretching isomerism as is known for Ba_3Ge_4. A study of different crystals shows a slight variation in the lattice parameters, suggesting the presence of a definite phase width which was substantiated by the successful synthesis of monophasic samples of $Sr_{3-x}Ca_xSn_5$ ($0.5 \leq x \leq 2.5$). However, all attempts to obtain the pure Ca phase, Ca_3Sn_5 have been unsuccessful. The compounds show a weakly metallic behavior, as shown by the electrodeless Q method. Magnetic studies show a very low susceptibility (nearly temperature independent till 5 K). Our studies suggest that the "Sn" polyanions in $Ca_{2.04}Sr_{0.96}Sn_5$ may be described as an arachno-Sn_5^{-6} Zintl cluster.

Introduction

Research in the area of polar intermetallics has led to the discovery of several novel structures in the past.[1−4] These compounds, which are formed with electropositive elements (alkali and alkaline earth) and the elements on the Zintl border, display many structural features that require understanding of the new concepts such as metallic Zintl phases[5,6] and the effects of packing and nonclassical bonding.[7−9] The alkaline earth−tin system has been of interest among various groups. The common structures in this system are CaSn,[10] Ca_2Sn,[10] $Ca_{31}Sn_{20}$,[11] SrSn, Sr_2Sn, Sr_5Sn_3, $SrSn_3$, $SrSn_4$, and more recently, Sr_3Sn_5, reported in the Sr−Sn system.[12] In the recent past, a fairly good amount of work has been done to investigate effects of cations on the Zintl anions.[13−15] A strong relationship between the polyanion E_n^{m-} formed and the type of cations surrounding it was established. Sr_3Sn_5 is known to crystallize in the Pu_3Pd_5 structure type (orthorhombic, C*mcm*, $Z = 4$).[16] This structure type is known to be adapted by many alkaline and rare earth tetrel systems, such as Ba_3Pb_5, La_3Sn_5,[17] and Ba_3Sn_5,[18] and rare earth triel systems, such as La_3In_5 and β-Y_3In_5.[19] In these triel systems, a well-defined interconnected network of square pyramids of indium could be recognized. Significant In−In bonding in these structures leads to the In_5^{-9} clusters described as a closed-shell nido-deltahedron.[19] The role of cations on the formation of the anionic substructure has been well studied. The size of the cations and their polarizing power (charge) seems to affect the formation of different Zintl polyanions. Mg^{2+} ions, for example, with their small size, lead to a highly

* To whom correspondence should be addressed. Phone: 91-11-26591511. Fax: 91-11-26854715. E-mail: ashok@chemistry.iitd.ernet.in.

(1) Corbett, J. D. *Inorg. Chem.* **2000**, *39*, 5871.
(2) Corbett, J. D. *Angew. Chem., Int. Ed.* **2000**, *39*, 670.
(3) Corbett, J. D. In *Chemistry, Structure and Bonding of Zintl Phases and Ions*; Kauzlarich, S., Ed.; VCH: New York, 1996; Chapter 3.
(4) Schaefer, H. *Annu. Rev. Mater. Sci.* **1985**, *15*, 1.
(5) Nesper, R. *Prog. Solid State Chem.* **1990**, *20*, 1.
(6) Nesper, R. *Angew Chem., Int. Ed. Engl.* **1991**, *30*, 789.
(7) Corbett, J. D.*Chem. Rev.* **1985**, *85*, 383.
(8) Sevov, S. C.; Corbett, J. D. *Inorg. Chem.* **1991**, *30*, 4875.
(9) Dong, Z.-C; Corbett, J. D. *J. Am. Chem. Soc.* **1994**, *116*, 3429.
(10) Eckerlin, P.; Meyer, H. J.; Wolfel, E. Z. *Anorg. Allg. Chem.* **1955**, *281*, 322.
(11) Ganguli, A. K.; Guloy, A. M.; Leon-Escamilla, E. A.; Corbett, J. D. *Inorg. Chem.* **1993**, *32*, 4349.
(12) Palenzona, A.; Pani, M. *J. Alloys Compd.* **2004**, *384*, 227.
(13) Currao, A.; Curda, J.; Nesper, R. *Z. Anorg. Allg. Chem.* **1996**, *622*, 85.
(14) Ganguli, A. K.; Corbett, J. D.; Köckerling, M. *J. Am. Chem. Soc.* **1998**, *120*, 1223.
(15) Li, B.; Chi, L.; Corbett, J. D. *Inorg. Chem.* **2003**, *42*, 3036.
(16) Cromer, D. *Acta Crystallogr.* **1976**, *B32*, 1930.
(17) Klem, M. T.; Vaughey, J. T.; Harp, J. G.; Corbett, J. D. *Inorg. Chem.* **2001**, *40*, 7020.
(18) Zürcher, F.; Nesper, R.; Hoffmann, S.; Fässler, T. F. *Z. Anorg. Allg. Chem.* **2001,** *627*, 2211.
(19) Zhao, J. T.; Corbett, J. D. *Inorg. Chem.* **1995**, *34*, 378.

10.1021/ic050677t CCC: $30.25
Published on Web 09/10/2005

charged anionic sublattice (cluster or isolated), whereas larger cations and others with low charge density lead to the coordination among anions. The effect of cations could well be appreciated by comparing the intercluster In−In distances in La_3In_5 and β-Y_3In_5, for which that of the former is distinctly greater than that of the latter.[19] This could be explained simply in terms of matrix effects wherein the separation between the clusters is directly related to the cation size. The intercluster bonding has an important bearing on the electronic properties of these compounds and could lead to the metallic behavior in compounds with significant cluster interaction as compared to the semiconducting behavior in the limit of no intercluster bonding. In Sr_3Sn_5, there is a tendency for the Sn clusters to be quite close to each other but not polymerizing through a covalent linkage. In the recent past, various examples of through-bond interactions leading to isomerism have been reported. Within the extended solid systems, Ba_3Ge_4[20] is one such well-studied example. The two isomers, both fulfilling the Zintl−Klemm concept and satisfying $8 - N$ rule, exist for this compound at different temperatures. Above 630 K, a phase isotypic with Ba_3Si_4 exists exclusively with isolated Ge_4^{6-} (butterfly shaped). As the temperature is lowered to room temperature, α-Ba_3Ge_4 gets stabilized with a chain like cross-linked polymer of the Ge_4^{6-} ion.[20] The formation of chains at low temperatures has been attributed to the size of Ba^{2+} ions, which is insufficient to keep the monomers far apart and stabilize them. It may be noted that this type of bond-stretching isomerism does not lead to any change in the charge on ions or the number of bonds. The effect of mixed alkali−metals on the stabilities of these ionic cluster salts in solids had not been studied earlier, although examples in this system with the mixed tetrel ions are known.[18] The effects of packing, as well as electronic effects from the random distribution of different cations, definitely seem to be important. In this article, we discuss the structure of a new compound, $Sr_{2.04(1)}Ca_{0.96(1)}Sn_5$, which shows an interesting structural distortion at low temperatures. We discuss the intercluster and intracluster variation of bond lengths and compare them with the bond stretching isomerism known in Ba_3Ge_4 and in the cyclic polysilanes.[21] We also report the synthesis and structural (single crystal and powder x- ray diffraction), electrical, and magnetic properties of the solid solution $Sr_{3-x}Ca_xSn_5$ ($0.5 \leq x \leq 2.5$).

Experimental Section

Syntheses. Nearly monophasic samples of $Sr_{(3-x)}Ca_xSn_5$ were obtained from the direct fusion of pure elements. Tin (Aesar 99.99%), strontium (Aesar 99.8%), and calcium (Aesar 99.9%) were weighed in a stoichiometric amount, loaded in Ta tubes, welded under a helium atmosphere, and then jacketed within fused-silica containers that were well flamed under high vacuum prior to sealing. All the metals were stored and handled in a helium-filled glovebox. The nominal composition of the loaded mixture from which the crystal of Sr_2CaSn_5 was obtained was $CaSrSn_3$. The reaction mixture was fired at 950° for 72 h and then cooled to room temperature at the rate of 5 °C per hour. After the crystal structure was solved, the exact composition was loaded to yield a monophasic compound. Similar conditions were used to obtain compounds of the type $Sr_{3-x}Ca_xSn_5$ ($0.5 \leq x \leq 2.5$).

X-ray Powder Diffraction. The powder diffraction patterns of all the above compounds were obtained from the Huber Guinier camera using Cu Kα1 radiation and were used for phase identification. Samples were mounted between two Mylar sheets using a block and ring assembly inside the nitrogen-filled box. The examination of the X-ray powder pattern of the initial reaction ($CaSrSn_3$) revealed approximately 30% $Sr_{2.04(1)}Ca_{0.96(1)}Sn_5$ phase. The presence of the title phase was established by matching the observed pattern with the generated pattern using the lattice parameters, space group, and the atomic positions from the single-crystal studies. Other phases observed were (Ca/Sr)Sn (20%) and Sn (50%). The stoichiometric reactions subsequently yielded nearly pure phases of $Sr_{3-x}Ca_x$ Sn_5 ($0.5 \leq x \leq 2.5$). The lattice parameters were refined from the powder patterns using PowderCell version 2.1[22]. We could not obtain the pure Ca phase, Ca_3Sn_5.

Single-Crystal Structure Determination. A few small blackish-gray crystals of the title compound were isolated from the parent mixture (loaded composition, $CaSrSn_3$) and placed inside a capillary (0.3 mm) under a nitrogen atmosphere. The capillaries were sealed and the crystals were checked for singularity. One of the crystals, with approximate dimensions of $0.09 \times 0.07 \times 0.07$ mm, was used for the X-ray crystallographic analysis. The X-ray intensity data were measured at two different temperatures (300 and 100 K) on a Bruker SMART[11] APEX CCD area detector system equipped with a graphite monochromator and a Mo Kα fine-focus sealed tube (λ = 0.71073Å) operated at 1500 W power (50 kV, 30 mA). The detector was placed at a distance of 4.995 cm from the crystal. For the room-temperature measurement, a total of 1800 frames were collected with a scan width of 0.3° in ω and an exposure time of 10 s/frame. The total data collection time was approximately 8 h. The frames were integrated with the Bruker SAINT software package[23] using a narrow-frame integration algorithm. The integration of the data using an orthorhombic unit cell yielded a total of 4242 reflections to a maximum θ angle of 28.30° (0.75 Å resolution), of which 645 were independent (completeness = 98.2%, R_{int} = 2.87%, R_{sig} = 1.93%**)** and 3638 reflections (86.5%) were greater than $2\sigma(I)$. Analysis of the data showed negligible decay during data collection. Data were corrected for absorption effects using the multiscan technique and SADABS.[24] We have also collected X-ray data at low temperature (100 K). A total of 1250 frames were collected at 100(2) K on the same crystal with a scan width of 0.3° in ω and an exposure time of 10 s/frame; 2757 reflections were observed with 617 reflections being independent (completeness = 54.3%, R_{int} = 2.29%, R_{sig} = 2.10%**)**. Data and refinement parameters at low temperature are given along with those at the room temperature in Table 1.

The structure was solved and refined using the Bruker SHELXTL (version 6.1) software package.[25] Out of the two possible space groups consistent with the extinctions, $Cmc2_1$ (noncentrosymmetric) and *Cmcm* (centrosymmetric), the latter was selected for the refinement. The choice was based on the mean $E^2 - 1$ value, which was close to the expected value for the centrosymmetric space group

(20) Zürcher, F.; Nesper, R. *Angew. Chem., Int. Ed.* **1998**, *37*, 3314.
(21) Schoeller, W. W.; Dabisch, T.;Busch, T. *Inorg. Chem.* **1987**, *26*, 4383.
(22) Kraus, W.; Nolze, G. *Powder Cell for Windows*, version 2.4; Federal Institute for Materials Research and Testing: Berlin, Germany, 2000.
(23) *SMART* and *SAINT*; Bruker AXS Inc.: Madison, WI, 1998.
(24) Sheldrick, G. M. *SADABS User Guide*; University of Göttingen: Göttingen, Germany, 1997.
(25) Sheldrick, G. M. *SHELXTL*, version 6.10; Bruker AXS Inc.: Madison, WI, 2001.

Table 1. Important Crystal Data and Structure Refinement at 300 and 100 K

empirical formula	$Ca_{0.96(1)}$ Sn_5 $Sr_{2.04(1)}$	$Ca_{0.96}$ Sn_5 $Sr_{2.04}$
fw	808.77	808.77
temp (K)	300	100(2)
cryst syst	orthorhombic	orthorhombic
space group, Z	*Cmcm*, 4	*Cmcm*, 4
unit cell dimensions		
a (Å)	10.5178(9)	10.4659(16)
b (Å)	8.4789(8)	8.4256(13)
c (Å)	10.7622(10)	10.6972(16)
density$_{calcd}$ (Mg/m^3)	5.597	5.695
abs coeff (mm^{-1})	24.273	24.696
final R indices[a]		
$I>2\sigma(I)$	R1 = 0.0156	R1 = 0.0289
	wR2 = 0.0319	wR2 = 0.0808
all data	R1 = 0.0168	R1 = 0.0312
	wR2 = 0.0321	wR2 = 0.0822

[a] $R_1 = \Sigma(|F_o - F_c|)/\Sigma(|F_o|)$. $wR2 = [\Sigma w(F_o^2 - F_c^2)/\Sigma wF_o^4]^{1/2}$. $GOF = [\Sigma w(F_o^2 - F_c^2)/(n - p)]^{1/2}$ where n is the number of reflections and p is the number of parameters refined.

Table 2. Atomic Coordinates ($\times 10^4$) and Equivalent Isotropic Displacement Parameters (Å^2 $\times$ 10^3) at 300 and 100 K

	x	y	z	U(eq)[a]	occupancy
		300 K			
Sn(1)	2012(1)	2101(1)	2500	18(1)	1.0
Sn(2)	0	1861(1)	4487(1)	17(1)	1.0
Sn(3)	0	4612(1)	2500	16(1)	1.0
Sr(1)/Ca(1)	2974(1)	0	5000	16(1)	0.771/0.229(4)
Sr(2)/Ca(2)	0	−1450(1)	2500	15(1)	0.501/0.499(6)
		100 K			
Sn(1)	2025(1)	2104(1)	2500	11(1)	1.0
Sn(2)	0	1864(1)	4495(1)	11(1)	1.0
Sn(3)	0	4631(1)	2500	10(1)	1.0
Sr(1)/Ca(1)	2974(1)	0	5000	14(1)	0.771/0.229
Sr(2)/Ca(2)	0	−1435(2)	2500	16(1)	0.501/0.499

[a] U(eq) is defined as one-third of the trace of the orthogonalized U_{ij} tensor.

and a better combined figure of merit, with $Z = 4$ for the formula unit, $Sr_{2.04(1)}Ca_{0.96(1)}Sn_5$. Three systematic absence violations were observed but were very weak in intensity. The structure was solved with SHELXS[26] using direct methods. All of the positional coordinates were revealed correctly in the initial solution given by SHELXS.[26] Refinement of the initial model with three Sn and two Sr atoms with all the sites fully occupied led to somewhat high U(eq) for Sr1 and Sr2. This suggested a less than full occupancy at these sites. Subsequently, both of these Sr sites were refined along with Ca, which led to approximately 77% and 50% Sr occupancies at the 8e and 4c sites, respectively (Table 2), the rest being occupied by Ca. The final anisotropic full-matrix least-squares refinement on F^2 with 29 variables converged at R1 = 1.68%, for the observed data and wR2 = 3.21% for all data. The details of the refinement have been given in Table 1. The refinement of the low-temperature data proceeded in a similar fashion using SHELXTL.[25] Although five weak systematic absence violations were observed, the structure could be refined in the *Cmcm* space group satisfactorily. A distinct contraction in the lattice parameters was observed, which led to the deviation in occupancies of Sr and Ca as compared to that at room temperature. In the final refinement, the occupancies of both of the mixed sites were fixed according to that refined from the room-temperature data. This led to a marginal increase in the isotropic thermal parameters of the mixed cations and wR2 with an overall better goodness of fit. No significant effect of this constraint was observed on the Sn positions and their thermal parameters.

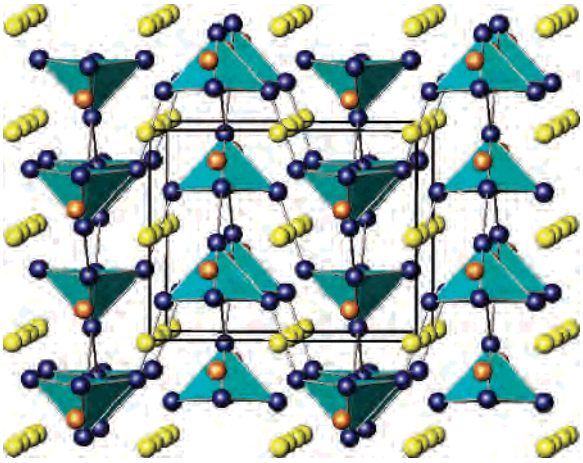

Figure 1. ~[001] view of the orthorhombic structure of $(Ca/Sr)_3Sn_5$ at 300 K. Sn atoms are shown in blue and Sn square pyramids are shown in green. The two mixed alkali metal sites are shown in yellow (Sr1/Ca1) and orange (Sr2/Ca2), respectively. Two types of intercluster contacts can be seen: Sn2−Sn2 (thin) and Sn1−Sn3 (thick) bonds.

Physical Properties. Electrical resistivity of nearly single-phase (>95%) samples of $Sr_{3-x}Ca_xSn_5$ ($0.5 \le x \le 2.5$) were measured at 34 MHz by the electrodeless Q method over a range of 110−294 K.[19] The powdered sample that had been sieved to a grain size between 150 and 250 μm was dispersed in chromatographic Al_2O_3. The absolute resistivity (extrapolated to 298 K) of $Sr_{3-x}Ca_xSn_5$ for $x = 0.5$ and 1.0 was found to be 35 and 45 $\mu\Omega$ cm, respectively, compared to 11 $\mu\Omega$ cm for Sr_3Sn_5. The former ($x = 0.5$) showed a temperature-independent behavior for ρ, while the latter ($x = 1.0$) was weakly metallic. The magnetic susceptibility of these samples was obtained at a field of 3 T over a range of 6−300 K with the aid of a Quantum design (MPMS) SQUID magnetometer. Samples were accurately weighed and were held between two fused silica rods within a tightly fitting outer silica tube and sealed under helium.[27] The raw data were corrected for the susceptibility of the container and the diamagnetic contributions of the ion cores.

Results and Discussion

$Sr_{2.04(1)}Ca_{0.96(1)}Sn_5$ was found to crystallize in the Pu_3Pd_5 structure type with the occurrence of square pyramidal clusters of Sn atoms typical for this structure type. The ~[001] view of the $Sr_{2.04(1)}Ca_{0.96(1)}Sn_5$ unit cell at room temperature is shown in Figure 1. Both alkali metal sites were found to be randomly mixed, and no site preference for any cation was observed. All attempts to synthesize pure Ca_3Sn_5 were unsuccessful probably because of the destabilizing effect of the small Ca ions on the Sn_5 cluster. This led us to determine the solubility of Ca ions in Sr_3Sn_5. We could obtain the solid solution until $x = 2.5$, leading to the most Ca-rich composition, $Sr_{0.5}Ca_{2.5}Sn_5$. This gives the clear indication of the role played by the surrounding cations on the stability of the polyanions and the structure at large.

Structural Distortion at Low Temperature. The absence of the pure Ca-compound Ca_3Sn_5 while the Sr-rich compound exists leads us to ponder the size effect, the chemical pressure being exerted by small cations. To understand the matrix

(26) Sheldrick, G. M. *SHELXS-97*; University of Göttingen: Göttingen, Germany, 1997.

(27) Sevov, S. C.; Corbett, J. D. *Inorg. Chem.* **1992**, *31*, 1895.

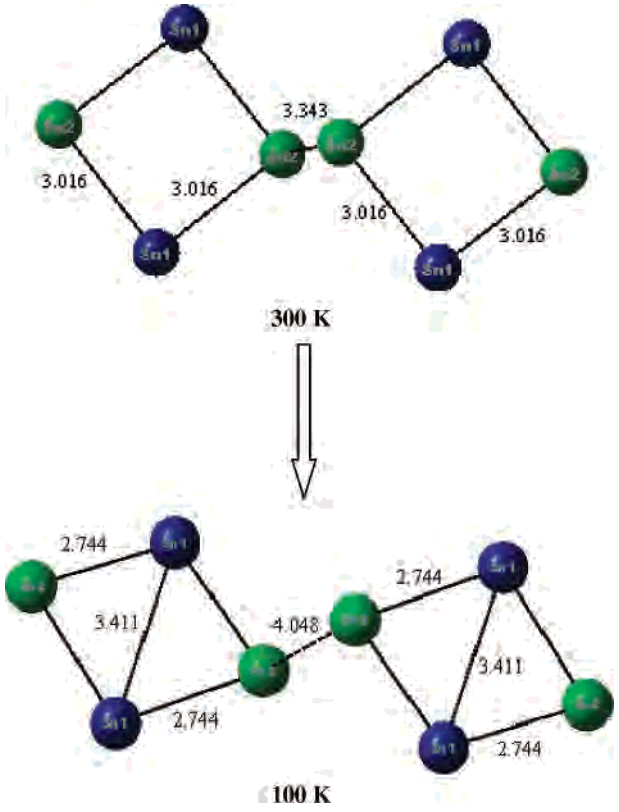

Figure 2. Base to base intercluster connectivity between two Sn polyanions at room temperature and at 100 K.

effects in this mixed alkaline-earth stannide, we carried out a low-temperature single-crystal diffraction study. A distinct structural distortion was observed when the crystal was cooled to 100 K. A slight contraction along all the three axes was observed. The overall structure remains the same with major changes observed in the Sn_5^{6-} polyanionic substructure. The disposition of the Sn atoms forming the base of square pyramids is compared at room temperature and 100 K in Figure 2. An approximately 20% increase in the intercluster Sn−Sn distance can be clearly seen. The distortion in the Sn polyanion at low temperature is manifested in the changes in the intracluster distances shown in Figure 4. Whereas at room temperature the intercluster bond d(Sn2−Sn2) (base to base, 3.34 Å) is shorter than the intercluster bond d(Sn1−Sn3) (base to apex, 3.78 Å), the former gets elongated (4.05 Å) and the latter contracts by ∼0.18 Å at 100 K (compare intercluster distances in Figures 2 and 3). Table 3 lists the important angles between the Sn atoms constituting the cluster. As indicated by the Sn2−Sn3−Sn2 and Sn1−Sn3−Sn1 angles that constitute the vertex of the polyhedra, the cooling of the crystal leads to an unequal contraction in the vertex angles with a reduction of 8° for the former and 24° for the latter. This forces the basal Sn2 atoms away and opens up the Sn2−Sn1−Sn2 angle by 30°. The opening of Sn2−Sn1−Sn2 bond is accompanied with the contraction of one of the intracluster Sn1−Sn2 bonds (2.74 Å) which is shorter than the Sn−Sn bond in metallic Sn (metallic radii of Sn 1.45 Å). These two factors perhaps lead to an increase in the intercluster Sn2−Sn2 distance, however it is not enough to destabilize the polyanionic substructure.

All of the Sn−Sn distances in the Sn polyhedra are quite close to the Sn−Sn single bond (d(Sn−Sn) = 2.91Å) with two notable exceptions. A longer bond, d(Sn−Sn) = 3.343 Å, is observed for the Sn2−Sn2 (base to base) intercluster distance at room temperature, whereas a short Sn−Sn distance, d(Sn−Sn = 2.74 Å), between basal Sn1 and Sn2 is observed at 100 K (Table 4). Comparing the intercluster distances (at 300 K) of Sr_3Sn_5 and $Sr_{2.04(1)}Ca_{0.96(1)}Sn_5$, we observed that the base to base (Sn2−Sn2) and base to apex (Sn1−Sn3) distances in Sr_3Sn_5 contract by 0.07 and 0.08 Å, respectively, in $Sr_{2.04(1)}Ca_{0.96(1)}Sn_5$. This is in good agreement with the smaller size of the Ca ions compared to the size of Sr. Other intracluster Sn−Sn bond distances corroborate well in the two compounds. A slight reduction in the average bond distance between the alkali metal and Sn atoms is also observed in the mixed cation compound with the maximum and the minimum bond lengths being shorter by 0.08 and 0.06 Å, respectively.

A complete phase transformation has been reported in the case of Ba_3Ge_4[20] where the two forms exist at different

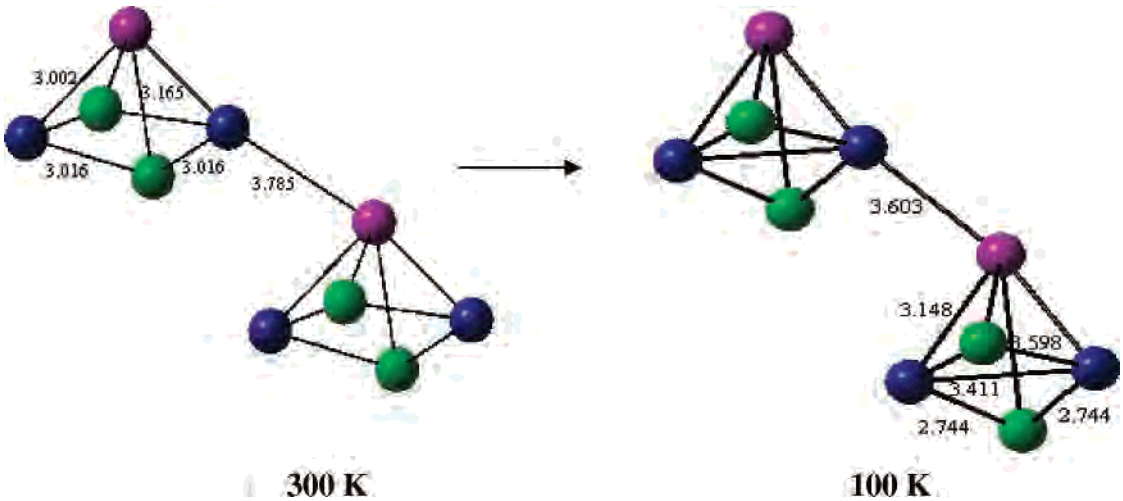

Figure 3. Base to apex intercluster connectivity between two Sn polyanions at room and at 100 K. The blue, green, and magenta represent the Sn1, Sn2, and Sn3 atoms, respectively.

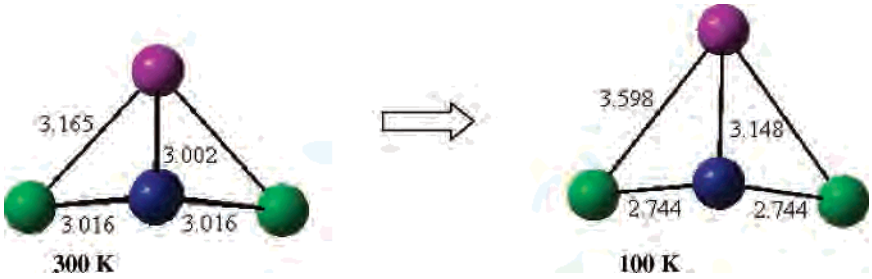

Figure 4. Sn polyhedra viewed along the *a* axis. Square pyramids stretch along the *b* axis and contract along the *c* axis when cooled to 100 K. The blue, green, and magenta represent the Sn1, Sn2, and Sn3 atoms, respectively.

Table 3. Selected Bond Angles (deg)

	Sn2−Sn1−Sn2	Sn2−Sn3−Sn2	Sn1−Sn3−Sn1
room temp	90.33	85.01	89.65
100 K	120.14	77.77	65.62

Table 4. Selected Bond Lengths (Å) at 300 and 100 K

	room temp	100 K
Sn(1)−Sn(2)	3.0156(4)	2.7437(6)
Sn(1)−Sn(3)	3.0020(5)	3.1475(10)
Sn(2)−Sn(3)	3.1649(5)	3.5081
Sn(1)−Sn(3)[a]	3.7853	3.6028

[a] Intercluster distances.

temperatures. The β-Ba_3Ge_4, isotypic with Ba_3Si_4, is stable only above 630 K, whereas α-Ba_3Ge_4 stabilizes at room temperature. The two phases are not isotypic, with α form crystallizing in a different structure type. The high temperature β phase is formed exclusively from isolated Tt_4^{-6} butterfly anions, which get cross-linked to form a chainlike polymer in α-Ba_3Ge_4. This has been referred to as bond-stretching isomerism.[20] Although we observe changes in intercluster distances in $Sr_{2.04(1)}Ca_{0.96(1)}Sn_5$ similar to those in Ba_3Ge_4, no phase transition to a different structure (or a different space group) was observed. Nearly monophasic samples of solid solution ($Sr_{3-x}Ca_xSn_5$) have also been synthesized. However, the reaction of Mg, Sr, and Sn ($Sr_{3-x}Mg_xSn_5$) under these conditions did not yield similar phases. Instead, Sr_3Sn_5 was obtained as the major phase (70%) along with 15% Sn and another phase (15%) related to $(Mg/Sr)_2Sn$ (*Pnma*, $a = 4.776$ Å, $b = 8.026$ Å, $c = 8.798$ Å, to be published). This strongly suggests that a cation with a large ionic radius is essential for the stability of this structure. It may be noted that even for the reactions where all the three alkaline-earth cations (Mg, Ca, and Sr) were used, for example, for the loaded compositions, $CaMgSrSn_3$ and $CaMg_2SrSn_3$, no Mg compound crystallized with the Pu_3Pd_5 structure type, which suggests a strict requirement for a larger cationic size for the stability of this structure. This may be true with the anionic substructure as well, as the exchange of tin and germanium leads to change from the M_3X_5 to M_3X_4 (M= Ba, Sr; X= Sn, Pb) structure.[18] This effect was however suggested to be the result of the maximal charge acquisition property of the Zintl anions of heavier and lighter tetralides. In the later cases, $(Mg/Sr)_2Sn$ (25% and 55%, respectively) were obtained along with $(Ca/Sr)_3Sn_5$ (45% and 15%, respectively) and rest as unreacted Sn. The lattice parameters for the compounds with $x = 0.5-2.5$ (which could be obtained as single phase compounds) were

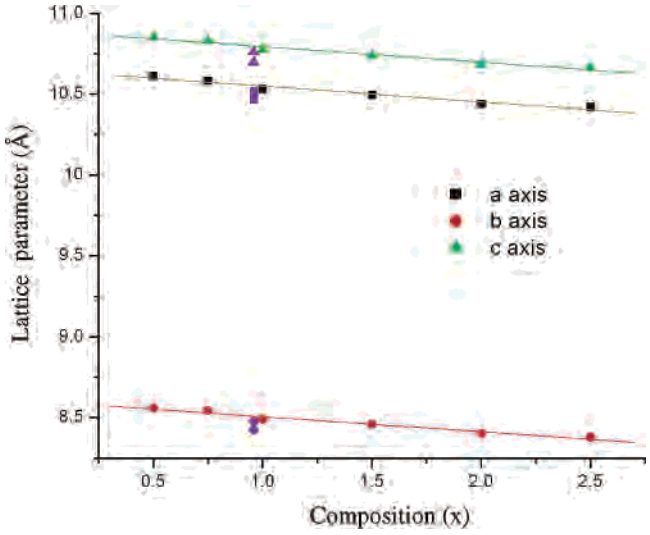

Figure 5. Plot of the variation of refined lattice parameters *a*, *b*, and *c* for $Sr_{3-x}Ca_xSn_5$ ($0.5 \le x \le 2.5$) with *x*. The two points in purple for each curve represents the single-crystal data at room temperature and at 100 K; the low-temperature data was refined with the fixed occupancy.

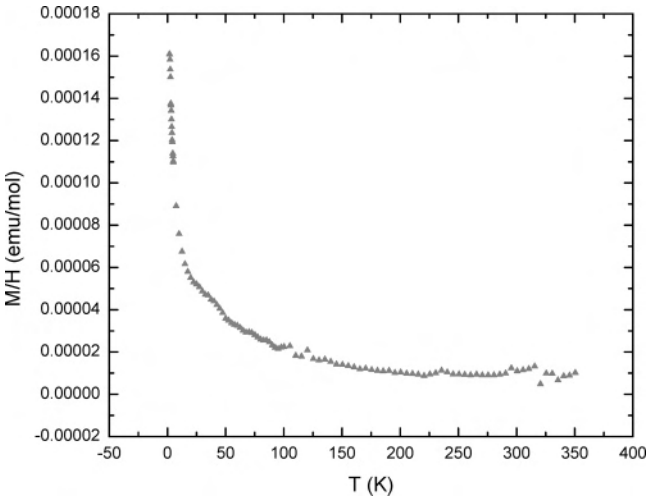

Figure 6. Molar magnetic susceptibility as a function of temperature at 30 kOe.

refined using PowderCell.[22] The variation in the lattice parameters as a function of *x* is shown in Figure 5. The lattice parameters (*a*, *b*, and *c*) are found to decrease continuously with increasing *x* as expected because of the smaller cationic size of Ca. Barring less than 10% impurity (Sn) in the case of $x = 1.0$ and 0.75 and 2−3% in the case of $x = 0.5$, the samples were nearly monophasic. However, there was no indication of the Pu_3Pd_5 type of phase in the pure Ca−Sn

mixture loaded in that stoichiometry; (~70% $CaSn_3$ and ~30% CaSn were obtained as the product). No single crystal could be obtained form the reaction mixture. As suggested by the resistivity experiments, incorporation of Ca leads to a higher absolute resistivity at room temperature compared to that of Sr_3Sn_5. The weak dependence of resistivity on the temperature in the case of $Ca_{0.5}Sr_{2.5}Sn_5$ is suggestive of a very weak metallic character which is also supported by the magnetic measurements. It may be noted that Sn_3Sn_5 was reported to be metallic earlier.[17] Figure 6 shows that the magnetic susceptibility is very small and nearly independent of the temperature down to ~50 K below which it increases, probably because of metallic impurities. From our resistivity and magnetic measurements of $Ca_{2.04}Sr_{0.96}Sn_5$, we believe it is close to a Zintl phase, and hence, the description of the Sn_5^{6-} clusters as an arachno species, allowing $Ca_{2.04}Sr_{0.96}Sn_5$ to be electron precise, appears to be more appropriate. This interpretation of electron precise 26 e-Sn_5^{-6} arachno clusters is explained by Wade-Mingos rules.[28,29] Zürcher et al.[18] have earlier described M_3Sn_5 (M= Sr, Ba) as arachno-type Sn_5^{6-} ion, although Sr_3Sn_5 appears to be better described as nido-Sn_5^{6-} since it was reported to be metallic.[17]

Acknowledgment. The authors thank the Department of Science and Technology, Government of India, and IIT Delhi for the funding of the Bruker SMART APEX X-ray diffractometer (with low-temperature facility). The authors also thank Professor J. D. Corbett, Iowa State University, for supporting (from his NSF Grant DMR-0129785) the visit of A.K.G. and S.G. to ISU, where part of this research was carried out.

Supporting Information Available: Additional crystallographic data and structure refinement parameters, anisotropic displacement parameters, and unique bond angles at 300 and 100 K. This material is available free of charge via the Internet at http://pubs.acs.org.

IC050677T

(28) Wade, K. *Chem. Commun.* **1971**, *792*, 7.
(29) Mingos, D. M. P. *Nature Phys. Sci.* **1972**, *99*, 236.